A prospective study of dual-energy CT in determining the metastatic and non-metastatic lymph nodes of colorectal cancer

Lin Qiu
The First Affiliated Hospital of Jinan University
Junjiao Hu
The First Affliated Hospital of Jinan University
Zeping Weng
The First Affliated Hospital of Jinan University
Fasheng Li
The First Affliated Hospital of Jinan University
Fei Wang
Jinan University First Affiliated Hospital
Sirun Liu
The First Affliated Hospital of Jinan University
Guangyu Jiang
The First Affliated Hospital of Jinan University
Xiangran Cai (caixran@jnu.edu.cn)
Jinan University First Affiliated Hospital https://orcid.org/0000-0003-4010-7577

Research article

Keywords: Computed tomography, Dual-energy spectrum imaging, Colorectal cancer, Lymph node

Posted Date: August 1st, 2020

DOI: https://doi.org/10.21203/rs.3.rs-44884/v1

Abstract

Background

To explore the ability of Dual-energy CT (DECT) to differentiate metastatic from non-metastatic lymph nodes in colorectal cancer (CRC).

Methods

Seventy-one patients with primary CRC underwent contrast-enhanced DECT imaging before surgery. The colorectal specimen was scanned after surgery, and lymph nodes were matched to the pathology report. The DECT quantitative parameters were analyzed: dual-energy curve slope value(λ_{HU}), standardized iodine concentration (n$\triangle$HU), iodine water ratio (nIWR), electron density value (nρ_{eff}), and effective atom-number (nZ), for the metastatic and non-metastatic lymph node differentiation. Also, sensitivity and specificity analyses were performed by using receiver operating characteristic curve.

Results

One hundred and fifty lymph nodes including 66 non-metastatic and 84 metastatic lymph nodes were matched using the radiological-pathological correlation. Metastatic node had a significantly greater λ_{HU}, n$\triangle$HU and nIWR values than non-metastatic node in both arterial and venous phases ($P < 0.01$). The AUC, sensitivity and specificity were 0.80, 80.30% and 65.48% for λ_{HU}; 0.86, 69.70% and 95.24% for n$\triangle$HU; 0.88, 71.21% and 95.24% for nIWR in the arterial phase. No significant difference was found in electron density and effective Z value for differentiation.

Conclusion

Dual-energy CT quantitative parameters may be helpful in diagnosing metastatic lymph nodes of CRC.

Background

Colorectal cancer (CRC) is the third most common type of cancer and the fourth leading cause of cancer-related death worldwide in the western world[1]. Over the past ten years, 1.2 million new cases were recorded[2, 3].Although its incidence in China is lower than that in the western countries, CRC has increased due to changes of life style in recent years and become a substantial cancer burden in China, particularly in the urban areas[4]. Lymph node metastasis is considered to be a risk factor for local recurrence and a poor prognosis in non-metastatic CRC[5]. Many studies revealed that the 5-year overall survival rate was 80%□90% for CRC patients without lymph node metastasis, compare to 60%~68% for those with nodal metastasis[6–8]. Also, a higher local recurrent rate is found in CRC patients with nodal

metastasis than in patients with negative nodes[9].The preoperative neoadjuvant therapy has been recommended by the National Comprehensive Cancer Network(NCCN) for the patients with positive lymph nodes, which could significantly reduce the risk of local recurrence and improve the survival rate[10].Therefore, accurate preoperative detection of lymphatic metastasis is essential for selecting the further treatment for these patients.

Currently, high-resolution MR imaging has been employed in an attempt to detect evidence of lymph node metastasis in CRC[11]. Also, functional MR techniques have been used to evaluate the lymph node status in CRC, such as diffusion weighted imaging (DWI). Qiu L etal have applied intravoxel incoherent motion imaging (IVIM) for differentiating metastatic from non-metastatic nodes in patients with rectal carcinoma[12].And they found IVIM parameters may be helpful for differentiation. However, due to the limited spatial resolution of IVIM images and discrepant b-value numbers and its distribution from different studies[13], it still can't be directly used to predict the nodal involvement in the clinical practice.

Dual energy CT (DECT) is an advanced CT technique that evaluates tissues at different X-ray energies, enabling spectral evaluation and material tissue characterization[14].Various studies have increasingly been demonstrated the potential advantages of DECT for the evaluation of lung adenocarcinoma[15], lymph node metastasis in gastric cancer[16], liver lesions[17–19], pancreatic tumor[20] and the prediction of metastatic lymph nodes in head and neck cancer[21]. Nevertheless, the application of DECT in the diagnosis of lymphatic metastases in CRC has rarely been reported. The present study was designed to investigate whether the parameters of the biphasic contrast-enhanced DECT were beneficial to differentiate metastatic from non-metastatic lymph nodes in CRC.

Methods

Patients

The present study obtained approval from the ethics committee of our hospital, and all patients signed the informed consent after a full explanation of the nature of the study. 90consecutive patients with primary CRC were enrolled from May 2015 to March 2019. Inclusion criteria: (1) Patients were confirmed as CRC by biopsy. (2) Patients did not receive radiotherapy or chemotherapy before surgery. (3) Patients had no iodine allergic history and no symptoms of hyperthyroidism. From these, 19 cases were excluded due to the following reasons: (1) poor preparation of bowel(n=7), (2) poor intestinal filling (n=5), (3) metal artifacts caused by pelvic or lumbar surgery (n=3), and (4) presence of gas artifacts affecting observation (n=4). Ultimately, a total of 71 cases were included in this study, including 41 males and 30 females, aged 31-91 years, with a mean age of (59.3±14.1) years. Patients underwent dual-phasic contrast-enhanced DECT 1-3 days before surgery.

DECT scan

The day before the examination, the patients were given a light diet that does not easily produce gas and dregs. In the morning on the day of DECT examination, patients underwent cleansing enema in the ward

until the watery stool discharged. 400 ml~1000 ml warm water (according to the tolerance of patients) was injected into the rectum before scanning.

All examinations were performed using a single-source CT system (Aquilion ONE; Canon Medical Systems), equipped with 320-detector raw and covered 160 mm in the z-direction. This system is capable of rapidly switching tube voltage from 80 to 135 kV within 50 milliseconds and automatically adapting the corresponding tube current. All patients were scanned in the supine position and underwent a routine non-contrast CT scan with the scanning parameters (tube voltage of 140 kV, tube current of 112~187 mA, matrix of 512×512, FOV of 240 mm, the rotation speed of 0.35 s/rot, slice thickness of 0.5 mm, slice spacing of 0.5 mm, and the scanning scope ranged from the diaphragmatic dome to pubic symphysis). The dual-phasic contrast-enhanced scans were then performed using the dual energy mode. The scan parameters were as follows: matrix of512×512, FOV of 240 mm, the rotation speed of0.35 s/rot and slice thickness of 0.5 mm, volume scan.55-86 ml (1.0 ml/kg) of a nonionic iodinated contrast agent (Ultravist300; Schering) was then administered via the antecubital vein at a flow rate of3 ml/s by G22 needle through an automatic injector. The dual-phasic scans were obtained at 40 s (arterial phase) and 70 s (venous phase) centering the tumor after the start of the contrast injection, respectively. The third generation AIDR 3D iterative algorithm developed by Canon was used, and the effective dose was 5.39 ± 0.48 mSv.

Histological examination

After surgical resection of the colorectal tumor, each specimen was taken back to the department of radiology and again imaged using the same conventional non-contrast sequence in the coronal and transverse planes before the specimen was fixed with formalin. After scanning, the specimens were immediately fixed with 4% neutral formaldehyde and delivered for the pathological examination.

The image slices of the preoperative CT scan and the postoperative specimens were compared to locate and mark all correct topographical matching lymph nodes with a diameter greater than 4mm in a blinded fashion by two radiologists (L.Q. and X.R.C., with 9 and20years abdominal imaging experience, respectively) in consensus. The morphological features of each lymph node were recorded according to the CT characteristics, ie, short-axis diameter, shape, border, and density. Subsequently, the specimens were delivered to the Department of Pathology, where every marked lymph node was harvested by one radiologist (L.Q) and one pathologist (Z.P.W., with 10 years of experience in pathological diagnosis). Any mismatch found between specimen CT images and histological findings were recorded and excluded from the study. Finally, all good-matched lymph nodes were stained with hematoxylin & eosin and were placed under a microscope for observation of histological features by two pathologists (Z.P.W. and G.Y.J., with 20 years of experience in pathological diagnosis), so as to determine the presence of tumor deposit.

Data analysis

The dual-phasic image volumes were loaded into the DE postprocessing software in the display console (Canon Aquilion ONE, Canon Medical System). The DE software automatically generated 35~135Kev CT

values to form single-energy CT curve, dual-energy iodine, base material, electron density and atom number images. A region of interest (ROI) of 12~78 $mm^2$was drawn using a circular tool on each marked lymph node on the reconstructed 69-keV monochromatic images (Fig.1). ROI was chosen to cover the nodal parenchyma as large as possible. The obvious suspicious necrotic region or fatty hilum was avoided from the ROI to minimize the influence of potential errors. Each lymph node was measured thrice and a mean value was calculated. Another ROI was placed on the right iliac artery at the corresponding layer as a reference. All of the ROIs were automatically copied onto all dual-energy iodine, base material, electron density and atom number images to calculate iodine concentration value (△HU), iodine water ratio value (IWR), electron density value (ρ_{eff}) and atom number value (Z).Measurements were performed in a blinded fashion by another two independent radiologists (J.J.H. and S.R.L., with 3 and 32years abdominal imaging experience, respectively) .

Statistical analysis

The slope of the dual-energy curve was expressed as λ_{Hu}[22], which was calculated by λ_{HU}=（35KeV $_{HU}$－69KeV $_{HU}$）/34 KeV, where 35KeV $_{HU}$ and 69KeV $_{HU}$ were the CT values at 35 KeV and 69 KeV, respectively (Fig. 2). The △HU, IWR, ρ_{eff} and Z values of lymph nodes were normalized to values in the iliac artery to drive the normalized values: n△HU=$\triangle HU_{tissue}/\triangle HU_{artery}$, nIWR=$IWR_{tissue}/IWR_{artery}$, n$\rho_{eff}$=$\rho_{efftissue}/\rho_{effartery}$, and nZ=$Z_{tissue}/Z_{artery}$. The measurements were carried out separately by two observers, and the average values were obtained for statistical analysis.

Statistical analyses were performed using SPSS20.0 (IBM, Aromonk) and Medcalc (MedCalc Software, Acacialaan 22, B-8400) software. A difference with P<0.05 was considered statistically significant. Measurement data in accordance with normal distribution were expressed by . Bland-Altman plots and the intraclass correlation coefficient (ICC) were used to analyze the interobserver variability of λ_{HU}, n△HU, nIWR, nρ_{eff} and nZ values: poor (less than 0.40), fair (0.40–0.59), good (0.60– 0.74), and excellent (0.75–1.00). The DECT parameters for the non-metastatic and metastatic lymph nodes were analyzed separately using two-sample t test. And the DECT parameters with statistical significance were used to plot receiver operating characteristic (ROC) curves, in which the optimal cut-off values were obtained using the Maximum Youden's index method.

Results

Histopathological Results and Morphological Features

All patients underwent laparoscopic surgery or open surgery to completely remove the tumor and mesangium. The histological results of all patients showed 28 cases of poorly differentiated adenocarcinoma and 43 cases of moderately differentiated adenocarcinoma. In histopathology, we collected a total of 399 lymph nodes around the tumor. Because the lymph nodes with a diameter of less than 4 mm in the specimen could not be accurately matched with CT images, 249 lymph nodes without metastasis were excluded. At the end, we included 150 lymph nodes around the tissues for analysis. The

pathological tissue showed that number of metastatic lymph nodes and normal lymph nodes were 84 and 66, respectively. Figure 3 shows the representative images of normal and metastatic lymph nodes.

There were more metastatic lymph nodes in those with greater than 10 mm in short-axis diameter. Moreover, more metastatic nodes are heterogeneous. In addition, the incidence of lymph node metastasis around the tumor was higher in patients with T4 staging and poorly differentiated CRC. Table 1 shows the distribution of normal lymph nodes and metastatic lymph nodes in the short axis, morphology and pathology of the included studies.

Interobserver agreement

Table 1 summarizes the measurements of normal and metastatic lymph nodes by two observers. It was found that the two observers have a high consistency in all DECT parameters measured. The Bland–Altman plots for lymph node measurement are shown in Figure 4, we found that most of the points located around the average difference line and within the 1.96 SD difference range.

Dual-energy characteristics of non-metastatic and metastatic lymph nodes

The λ_{HU}, n$\triangle$HU value, nIWR values of metastatic nodes in the arterial and venous phases were significantly greater than those of non-metastatic nodes ($P < 0.01$). However, nρ_{eff} and nZ did not show significant differences between the metastatic and non-metastatic lymph nodes (Table 2).

The ROC curves of DECT parametric values (λ_{HU}, n$\triangle$HU and nIWR) in differentiating normal from metastatic lymph nodes are shown in Fig. 5 and Table 3. The ROC curves demonstrated that the AUC values of all DECT parameters in the arterial phase was greater than those in the venous phase. The AUC of the nIWR, n$\triangle$HU and λ_{HU} statistically decreased. nIWR had the highest AUC, while λ_{HU} had the lowest. ROC analysis was carried out to determine the threshold for each parameter to optimize both the sensitivity and specificity for differentiating normal from metastatic lymph nodes. When 0.11was used as a nIWR threshold value, the sensitivity and specificity were 71.21%and 95.24%, respectively. Using an n$\triangle$HU value cutoff of0.19, metastatic lymph nodes could be diagnosed with 69.70% sensitivity and 95.24% specificity. When3.02was used as the λ_{HU} threshold value, the sensitivity and specificity were 80.30%and65.48%, respectively.

Discussion

In our study, we employed DECT parameters to predict the nodal metastasis, which can provide additional functional parameters for assessment in addition to CT values. Our study demonstrated DECT parameters, nIWR, n$\triangle$HU and λHU values in the arterial phase, especially nIWR has a higher accuracy for differentiating non-metastatic from metastatic nodes in CRC, suggesting DECT may be a promising technique for N staging in CRC.

In the present study, the nIWR, n△HU and λHU values of metastatic lymph nodes were significantly greater than those of non-metastatic lymph nodes. Iodine concentration reflects the degree of contrast enhancement[23]. An increase of iodine content in metastatic lymph nodes could be due to the increased tumor-related angiogenesis, blood volume or vascular permeability within the metastatic lymph nodes[24]. Some prior studies also found the similar results on the metastatic lymph nodes from the gastric cancer[25], rectal cancer[26] and cervical cancer[27]. In metastatic lymph nodes, the histopathological changes of metastatic foci affect blood volume and vascular osmotic pressure. There are more blood vessels in the metastatic lymph nodes than the non-metastatic lymph nodes[22], which results in the more significant enhancement. However, a study from Liu Het al[28]had the different finding, who employed the maximal short axis and iodine content to distinguish the metastatic lymph nodes in the colon cancer. They found that the iodine content in the metastatic lymph nodes was lower than that in the non-metastatic lymph nodes. Accordingly, they believed that the number of vessels in the lymph nodes was reduced after metastasis.

The studies on electron density and effective atom number have rarely been reported in the recent years. Tatsugami[29] reported that the effective atom number and electron density value might be helpful for improving accuracy in radiotherapy treatment planning. Liu X et al[22]found that nZ value was significantly greater in metastatic lymph nodes than in non-metastatic lymph nodes in patients with papillary thyroid cancer. But they didn't mention the electron density in their study, which might be related to the instrument and the dependent parameters. However, in the present study, it was found that the atom number and electron density did not show significant difference for differentiation between metastatic and non-metastatic lymph nodes, which might be associated with the difference in the primary tumor, DECT scanner, or nodal size.

In the present study, it was found that nIWR were of significant value in differentiating metastatic and non-metastatic lymph nodes in ROC, followed by △Hu and λHU in the arterial and venous phases. Also, these values in the arterial phase showed a higher diagnostic efficiency than those in the venous phase. nIWR, n△HU and λHU are related to the iodine content. After administration of contrast materials, metastatic lymph nodes demonstrated different iodine uptake from the non-metastatic. Thus, these values in the arterial and venous phases could be useful for differentiation. This result is also supported by the study from Tatsugami et al[29]. Nevertheless, Tatsugami et al. found that the AUC under the ROC in the venous phase was greater than that in the arterial phase. They believed that the enhancement in the venous phase was caused by leakage of contrast agent into the extravascular space due to the injury of vascular endothelial cells. This meant that the venous phase was more conducive for identification of metastatic lymph nodes, which is different from our study. This discrepancy might be due to the different CT instrument. In our study, we performed DECT scan in 320-detector-row dynamic volume CT system, which has a z-coverage width of 160 mm and allow a faster acquisition of entire tumor in a single rotation without bed movement[30]. IWR, △HU and λHU represent the change of iodine content calculated using three-material decomposition. And this change in iodine content could be more easily detected by our CT system in the early stage of injection of contrast agent.

The present study has the following limitations. Firstly, those lymph nodes less than 4 cm in diameter weren't included in this study to ensure a one to one good-match among the vitro and vivo CT images. In addition, measurements on smaller lymph nodes would be rather hard due to the limited spatial resolution. Secondly, ROI was placed within each lymph node and cover the nodal parenchyma as large as possible in the current study. However, some tumor deposits are merely located in the subcapsular region of lymph node[31].Some measurements based on ROIs might be a bit bias. Thirdly, our study was limited to the adenocarcinoma of CRC because more than 90% of CRC are adenocarcinomas originating from epithelial cells of the colorectal mucosa. other rare types of CRC, such as neuroendocrine, squamous cell, adenosquamous, spindle cell and undifferentiated carcinomas weren't included.

Conclusion

In summary, quantitative DE parameters including dual-energy curve slope, iodine content and iodine water ratio demonstrated higher accuracy for differentiation of metastatic and non-metastatic lymph nodes in CRC. The iodine water ratio in the arterial phase could be more valuable for the identification of metastatic nodes in CRC.

Abbreviations

DECT: Dual-energy CT; CRC:colorectal cancer; λHU:dual-energy curve slope value; n△HU:standardized iodine concentration; nIWR:iodine water ratio; npeff:electron density value; nZ:effective atom-number; NCCN:National Comprehensive Cancer Network; DWI:diffusion weighted imaging; IVIM:intravoxel incoherent motion imaging; ROI:region of interest; ICC:intraclass correlation coefficient; ROC:receiver operating characteristic.

Declarations

Ethics approval and consent to participate

The Institutional Review Board of The First Affiliated Hospital of Jinan University approved this study. All patients provided written consent to participate in this study.

Consent for publication

All patients enrolled have signed the same informed form in this research. The consent included patients have their data and clinical imaging used for publication. This research has deidentified all information pertaining to patients.

Availability of data and materials

The datasets used and/or analyzed during the current study are available from the corresponding author on reasonable request.

Competing interests

The authors declare that they have no conflict of interest.

Funding

This study was funded by Chinese Fundamental Research Funds for the Central Universities (21619360), Guangdong University youth innovation talent program (2019KQNCX004) and Medical Scientific Research Foundation of Guangdong Province of China(B2018192).

Authors' contributions

LQ and JJH have drafted the work and substantively revised it; ZPW and GYJ conducted histopathological analysis and interpretation; FSL, FW and SRL conducted the study and collected important background data; XRC experimental design, analysis and interpretation. All authors have read and approved this version of the submitted manuscript and are personally accountable to their contributions.

Acknowledgements

Thanks to the authors Jing Wen and En-ying Zhang and Xiang-xiang Chen, advanced application specialist at Canon Healthcare CT research China, Guangzhou, for technical consulting for practicing the DECT protocol.

References

1. David Cunningham WA, Heinz-Josef Lenz HT, Lynch. Bruce Minsky, Bernard Nordlinger, Naureen Starling: **Colorectal cancer**. Lancet. 2010;375:1030–47.
2. Jemal A, Bray F, Center MM, Ferlay J, Ward E, Forman D. Global cancer statistics. Cancer J Clin. 2011;61(2):69–90.
3. Torre LA, Bray F, Siegel RL, Ferlay J, Lortet-Tieulent J, Jemal A. Global cancer statistics, 2012. Cancer J Clin. 2015;65(2):87–108.
4. Fan YC, Ning FL, Zhang CD, Dai DQ: **Preservation versus non-preservation of left colic artery in sigmoid and rectal cancer surgery**: **A meta-analysis**. *International journal of surgery* 2018, **52**:269–277.

5. Kim J, Huynh R, Abraham I, Kim E, Kumar RR. Number of lymph nodes examined and its impact on colorectal cancer staging. Am Surg. 2006;72(10):902–5.
6. Koca D, Binicier C, Oztop I, Yavuzsen T, Ellidokuz H, Yilmaz U. Prognostic factors affecting recurrence and survival in patients with locally advanced rectal cancer. Journal of BUON: official journal of the Balkan Union of Oncology. 2012;17(2):291–8.
7. Zeng W-G, Zhou Z-X, Wang Z, Liang J-W, Hou H-R, Zhou H-T, Zhang X-M, Hu J-J. Lymph Node Ratio is an Independent Prognostic Factor in Node Positive Rectal Cancer Patients Treated with Preoperative Chemoradiotherapy Followed by Curative Resection. Asian Pac J Cancer Prev. 2014;15(13):5365–9.
8. Miller ED, Robb BW, Cummings OW, Johnstone PA. The effects of preoperative chemoradiotherapy on lymph node sampling in rectal cancer. Dis Colon Rectum. 2012;55(9):1002–7.
9. Backes Y, Elias SG, Bhoelan BS, Groen JN, van Bergeijk J, Seerden TCJ, Pullens HJM, Spanier BWM, Geesing JMJ, Kessels K, et al. The prognostic value of lymph node yield in the earliest stage of colorectal cancer: a multicenter cohort study. BMC Med. 2017;15(1):129.
10. Huang L, Li TJ, Zhang JW, Liu S, Fu BS, Liu W. Neoadjuvant chemotherapy followed by surgery versus surgery alone for colorectal cancer: meta-analysis of randomized controlled trials. Medicine. 2014;93(28):e231.
11. Chen Y, Yang X, Wen Z, Lu B, Xiao X, Shen B, Yu S. Fat-suppressed gadolinium-enhanced isotropic high-resolution 3D-GRE-T1WI for predicting small node metastases in patients with rectal cancer. Cancer imaging: the official publication of the International Cancer Imaging Society. 2018;18(1):21.
12. Qiu L, Liu XL, Liu SR, Weng ZP, Chen XQ, Feng YZ, Cai XR, Guo CY. Role of quantitative intravoxel incoherent motion parameters in the preoperative diagnosis of nodal metastasis in patients with rectal carcinoma. Journal of magnetic resonance imaging: JMRI. 2016;44(4):1031–9.
13. Sun H, Xu Y, Xu Q, Shi K, Wang W. Rectal cancer: Short-term reproducibility of intravoxel incoherent motion parameters in 3.0T magnetic resonance imaging. Medicine. 2017;96(19):e6866.
14. Yu Z, Mao T, Xu Y, Li T, Wang Y, Gao F, Sun W: **Diagnostic accuracy of dual-energy CT in gout: a systematic review and meta-analysis**. *Skeletal radiology* 2018.
15. Jiang H, Li X. Correlation of dual-source computed tomography/dual-energy imaging with pathological grading of lung adenocarcinoma and its clinical value. Pakistan journal of medical sciences. 2017;33(6):1429–33.
16. Li J, Fang M, Wang R, Dong D, Tian J, Liang P, Liu J, Gao J. Diagnostic accuracy of dual-energy CT-based nomograms to predict lymph node metastasis in gastric cancer. European radiology. 2018;28(12):5241–9.
17. Yang CB, Zhang S, Jia YJ, Yu Y, Duan HF, Zhang XR, Ma GM, Ren C, Yu N. Dual energy spectral CT imaging for the evaluation of small hepatocellular carcinoma microvascular invasion. Eur J Radiol. 2017;95:222–7.
18. Yu Y, Lin X, Chen K, Chai W, Hu S, Tang R, Zhang J, Cao L, Yan F. Hepatocellular carcinoma and focal nodular hyperplasia of the liver: differentiation with CT spectral imaging. European radiology. 2013;23(6):1660–8.

19. Lv P, Lin XZ, Li J, Li W, Chen K. Differentiation of small hepatic hemangioma from small hepatocellular carcinoma: recently introduced spectral CT method. Radiology. 2011;259(3):720–9.
20. George E, Wortman JR, Fulwadhva UP, Uyeda JW, Sodickson AD. Dual energy CT applications in pancreatic pathologies. Br J Radiol. 2017;90(1080):20170411.
21. Zhao Y, Li X, Li L, Wang X, Lin M, Zhao X, Luo D, Li J. Preliminary study on the diagnostic value of single-source dual-energy CT in diagnosing cervical lymph node metastasis of thyroid carcinoma. Journal of thoracic disease. 2017;9(11):4758–66.
22. Liu X, Ouyang D, Li H, Zhang R, Lv Y, Yang A, Xie C. Papillary thyroid cancer: dual-energy spectral CT quantitative parameters for preoperative diagnosis of metastasis to the cervical lymph nodes. Radiology. 2015;275(1):167–76.
23. Chen X, Xu Y, Duan J, Li C, Sun H, Wang W. Correlation of iodine uptake and perfusion parameters between dual-energy CT imaging and first-pass dual-input perfusion CT in lung cancer. Medicine. 2017;96(28):e7479.
24. KA M. Tumour angiogenesis and its relation to contrast enhancement on computed tomography: a review. Eur J Radiol. 1999;30(3):198–205.
25. Zilai Pan LP, Bei Ding C, Yan H, Zhang L, Du B, Wang. Qi Song,, Kemin Chen FY: **Gastric Cancer Staging with Dual Energy Spectral CT Imaging**. PLOS ONE. 2013;8(2):e53651.
26. Al-Najami I, Lahaye MJ, Beets-Tan RGH, Baatrup G. Dual-energy CT can detect malignant lymph nodes in rectal cancer. Eur J Radiol. 2017;90:81–8.
27. Naresh KN. AYNAMB: Angiogenesis is redundant for tumour growth in lymph node metastases. Histopathology. 2001;38:466–70.
28. Liu H, Yan F, Pan Z, Lin X, Luo X, Shi C, Chen X, Wang B, Zhang H. Evaluation of dual energy spectral CT in differentiating metastatic from non-metastatic lymph nodes in rectal cancer: Initial experience. Eur J Radiol. 2015;84(2):228–34.
29. Fuminari Tatsugami M, Toru Higaki PhD, Kiguchi M, So Tsushima RT, MSc,Akira Taniguchi, Yoko Kaichi RT, MD,Takuji Yamagami, MD, and Kazuo Awai, MD: **Measurement of Electron Density and Effective Atomic Number by Dual-Energy Scan Using a 320-Detector Computed Tomography Scanner with Raw Data-Based Analysis**: **A PhantomStudy**. *TECHNICAL NOTE* 2014, **38**:824–827.
30. Imae THA, Nakagawa K, Ino K, Tanaka K, Okano Y, Sasaki K, Saegusa S, Shiraki T, Oritate T, Yano K, Shinohara H. Motion Analysis of Target in Stereotactic Radiotherapy of Lung Tumors Using 320-row Multidetector CT. Nihon Hoshasen Gijutsu Gakkai Zasshi. 2011;67(3):202–11.
31. Rizzo S, Radice D, Femia M, De Marco P, Origgi D, Preda L, Barberis M, Vigorito R, Mauri G, Mauro A, et al. Metastatic and non-metastatic lymph nodes: quantification and different distribution of iodine uptake assessed by dual-energy CT. European radiology. 2018;28(2):760–9.

Tables

Table 1. CT Features in 150 Lymph Nodes

CT imaging features	Lymph nodes (n)	Metastatic nodes (n)	Prevalence (%)	Non-metastatic nodes (n)	Prevalence (%)
Size					
4mm≥D≤5mm	17	7	41.18	10	58.82
5mm< D≤10mm	108	56	51.85	52	48.15
D>10mm	25	21	84.00	4	16.00
Shape					
Round	97	48	49.48	49	50.52
Elliptical	53	36	67.92	17	32.08
Border					
Well-defined	120	66	55.00	54	45.00
Ill-defined	30	18	60.00	12	40.00
Density*					
Homogeneous	110	54	49.09	56	50.91
Heterogeneous	40	30	75.00	10	25.00
T satging					
T_3 staging	117	58	49.57	59	50.43
T_4 staging	33	26	78.79	7	21.21
Differentiation					
poorly	63	46	73.02	17	26.98
moderately	87	38	43.68	49	56.32
D, the maximal short-axis diameter.					

*Density on the reconstructed 69-keV monochromatic images of artery phase.

Table 2 Dual-energy parameters of metastatic and non-metastatic lymph nodes in different phases

	Arterial phase				Venous phase			
	Non-metastatic lymph nodes	Metastatic lymph nodes	t	p	Non-metastatic lymph nodes	Metastatic lymph nodes	T	p
λ_{HU}	2.40±0.98	3.60±1.10	7.08	<0.01	2.58±0.94	3.72±1.21	6.27	<0.01
n△Hu	0.19±0.03	0.36±0.11	9.45	<0.01	0.28±0.11	0.43±0.13	7.23	<0.01
nIWR	0.10±0.06	0.24±0.11	8.91	<0.01	0.28±0.10	0.41±0.08	8.93	<0.01
$n\rho_{eff}$	0.89±0.07	0.89±0.06	-0.58	0.56	0.89±0.06	0.89±0.07	0.49	0.62
nZ	0.94±0.04	0.95±0.03	-1.97	0.05	0.96±0.46	0.94±0.04	-1.50	0.14

Table 3 The value of dual-energy parameters in the arterial and venous phases (λ_{HU}, n△HU, and nIWR)for the differentiation of metastatic and non- metastatic lymph nodes

	Arterial phase			Venous phase		
	λ_{HU}	n△HU	nIWR	λ_{HU}	n△HU	nIWR
AUC	0.80	0.86	0.88	0.76	0.79	0.83
Maximum yoden index	0.46	0.65	0.68	0.38	0.45	0.52
Sensitivity	80.3	69.7	71.21	56.06	53.03	65.15
Specificity	65.48	95.24	95.24	82.14	91.67	94.05
Positivepredictive value	64.63	92	92.31	71.5	83.33	89.58
Negative predictive value	80.88	80	81.63	70.41	70.3	77.45
Cut-off point	3.02	0.19	0.11	2.56	2.3	0.28

Figures

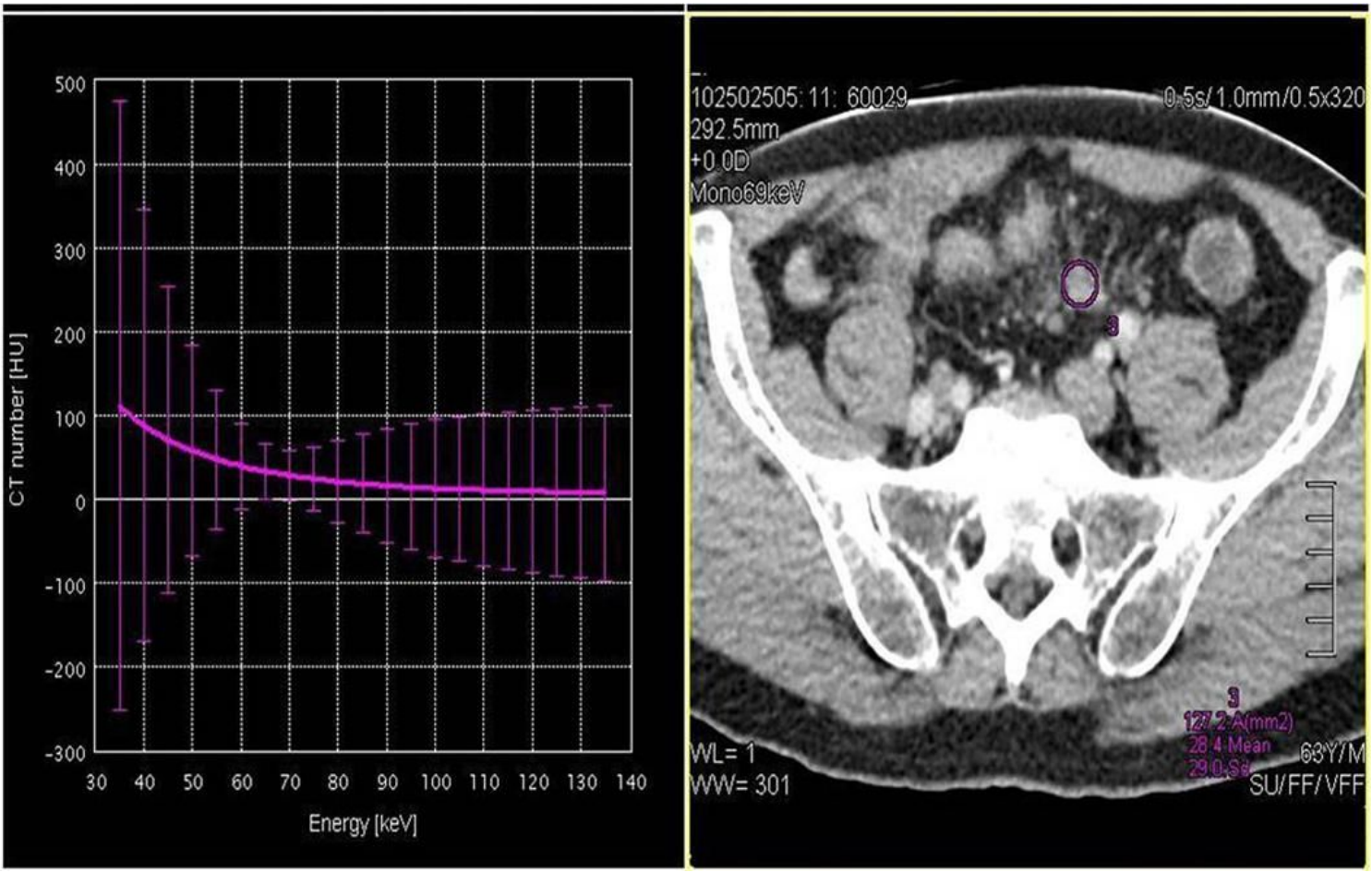

Figure 1

Measurement of lymph nodes; a. dual-energy CT curve; b. 69-keV monochromatic image.Measurement using the tools contained in the system. ROI was selected on lymph node and included the whole lymph node as much as possible.

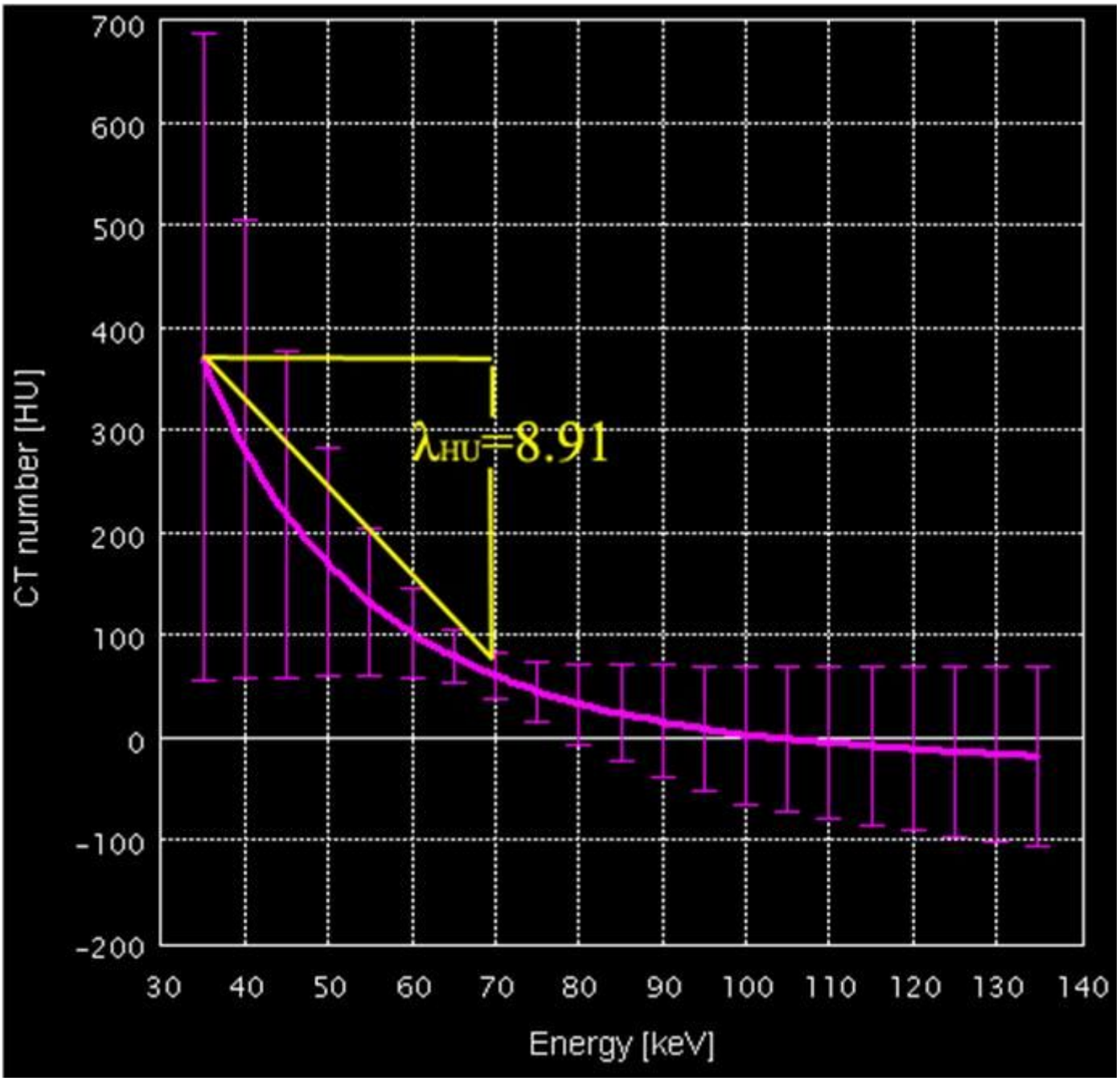

Figure 2

The calculation method for the slope of the ROI curve is shown. The pink line is a dual-energy CT curve; the slope of the curve in the region of interest is 8.91.

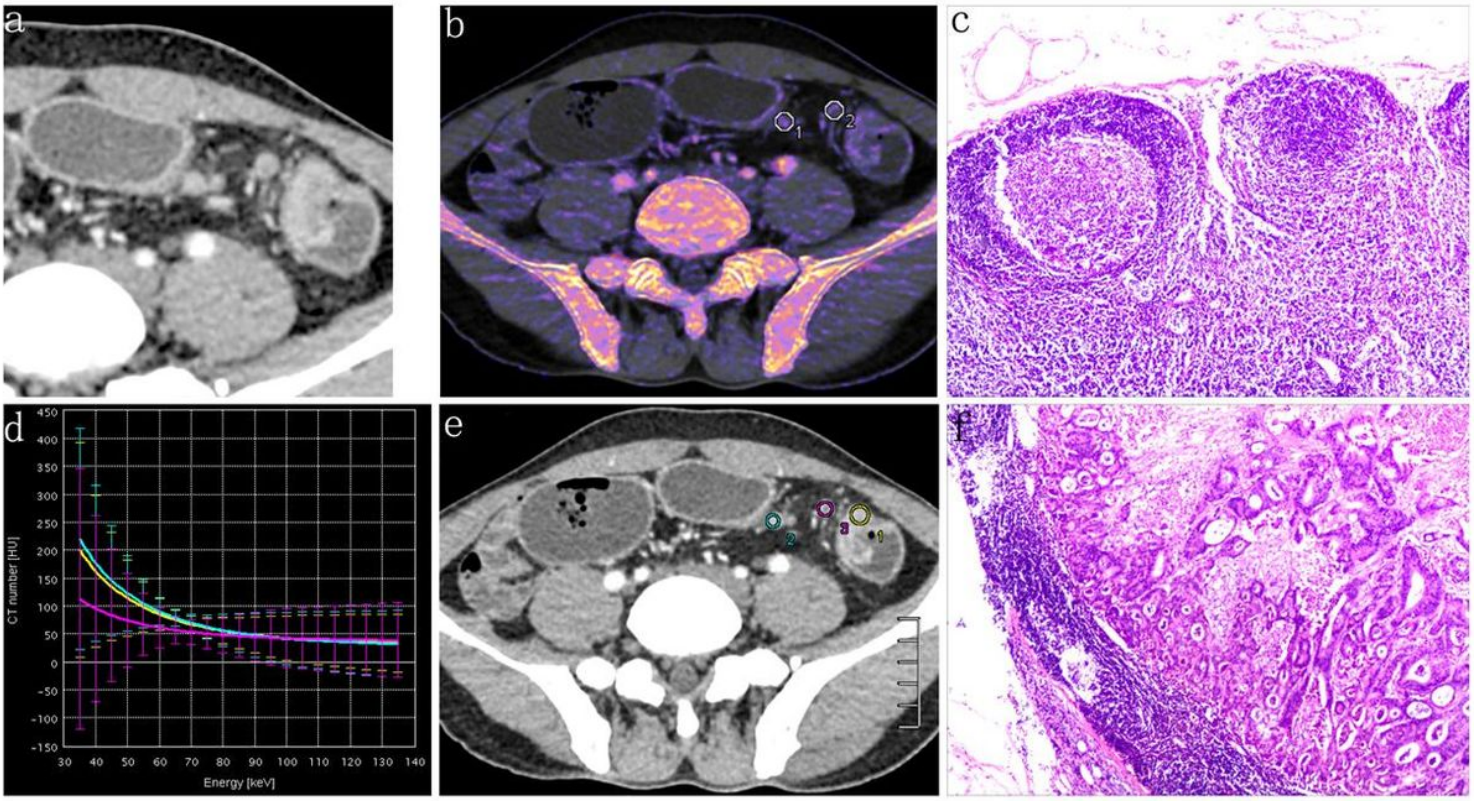

Figure 3

A 41-year-old man with colon cancer.a. Monochromatic obtained at 69 Kev energy level with the best signal-to-noise ratio: a mass shallow is visible in the descending colon (yellow arrow), with multiple lymph nodes in different sizes; b. Dual-energy iodine image; e. Dual-energy curve: the dual energy curve of the tumor (yellow line) almost overlaps with that of metastatic lymph node (blue line), with the same slope. The slope of the non-metastatic lymph nodes (pink line) is smaller than that of the metastatic lymph node(blue line);c and g: histopathological staining (HE staining, ×40). c: normal lymph node structurewith clear lymph follicles (△), g: the lymph follicles are replaced by cancer tissue (□).

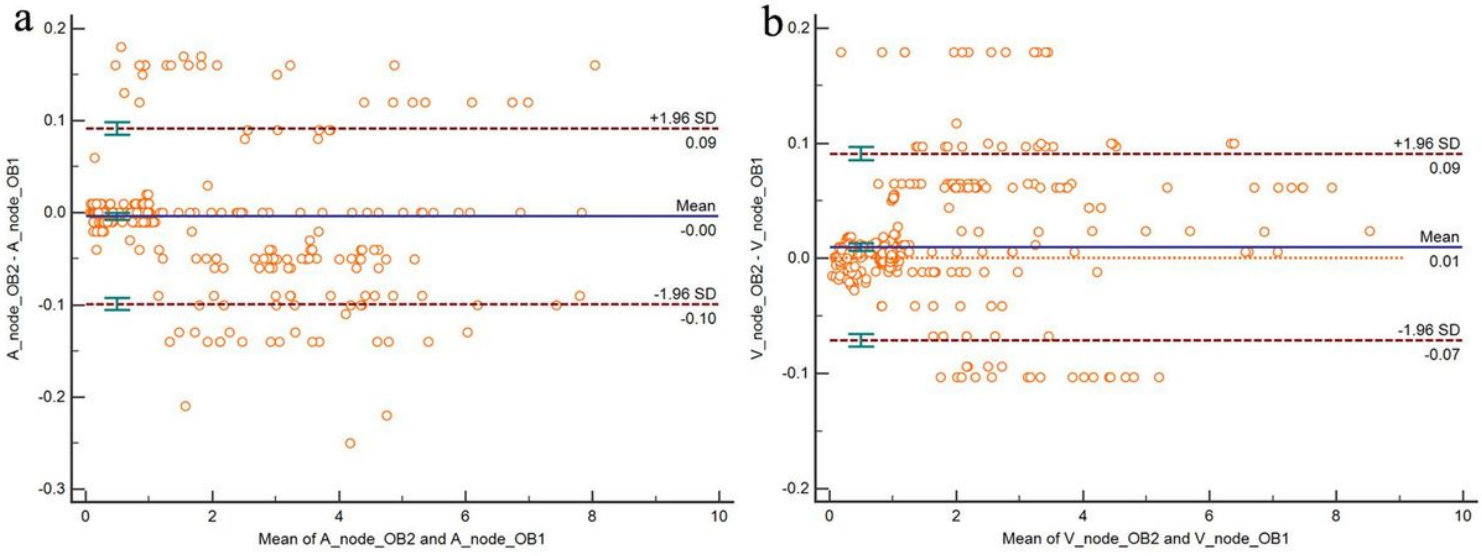

Figure 4

Bland-Altman scatter diagram of dual-energy parameters in the arterial phase; a. and venous phase; b. the solid line in the middle refers to the mean of the differences of values measured by two observers, the upper and lower dotted lines represent 95% confidence interval. The two diagrams show good repeatability in measuring various dual-energy parameters of the lymph nodes surrounding the colorectal cancer in the arterial and venous phases.

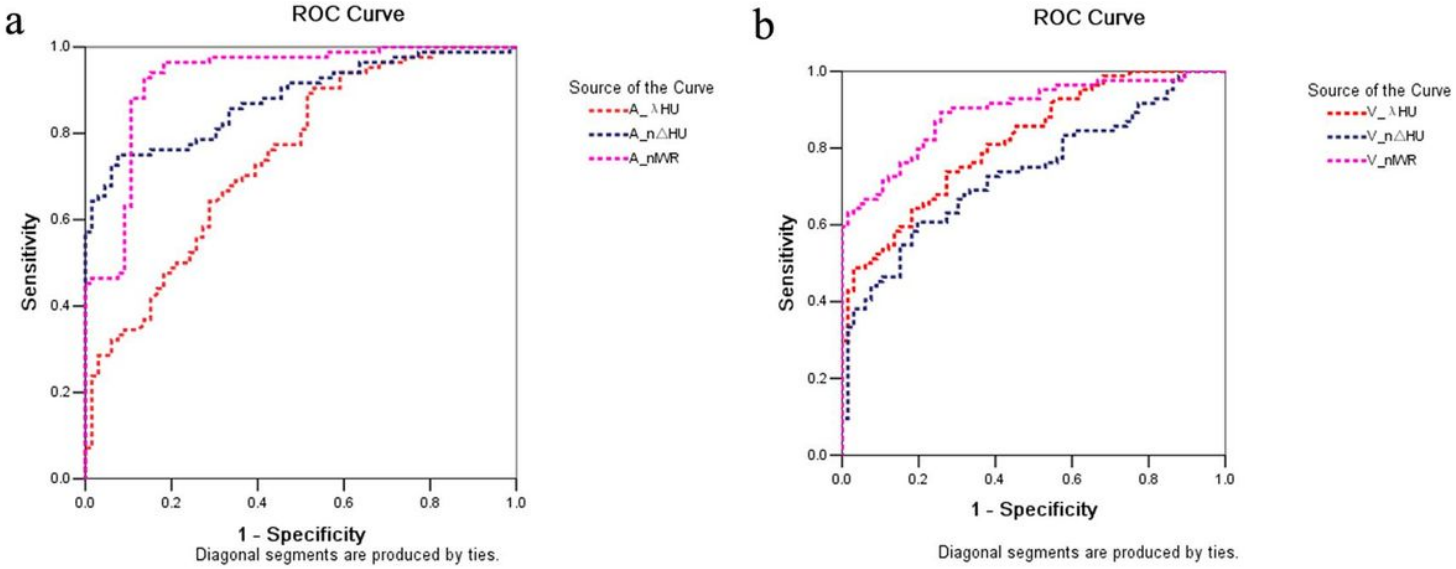

Figure 5

ROC curves for dual-energy parameters λHU, n△HU and nIWR in the differentiation of metastatic and non-metastatic lymph nodes; a. ROC curves in the arterial phase: nIWR value presents the highest diagnostic efficiency, followed by n△HU and λHU values;b. ROC curves in the venous phase: nIWR value displays the highest diagnostic efficiency, followed by λHu and n△HU values.